Plasma Chem Plasma Process (2016) 36:185–212
DOI 10.1007/s11090-015-9662-5

ORIGINAL PAPER

Plasma-Surface Interactions in Plasma Catalysis

Erik C. Neyts[1]

Received: 14 July 2015 / Accepted: 12 September 2015 / Published online: 16 October 2015

Abstract In this paper the various elementary plasma—surface interaction processes occurring in plasma catalysis are critically evaluated. Specifically, plasma catalysis at atmospheric pressure is considered. The importance of the various processes is analyzed for the most common plasma catalysis sources, viz. the dielectric barrier discharge and the gliding arc. The role and importance of surface chemical reactions (including adsorption, surface-mediated association and dissociation reactions, and desorption), plasma-induced surface modification, photocatalyst activation, heating, charging, surface discharge formation and electric field enhancement are discussed in the context of plasma catalysis. Numerous examples are provided to demonstrate the importance of the various processes.

Keywords Plasma catalysis · Plasma-surface interactions · Atmospheric pressure plasma · Dielectric barrier discharge (DBD) · Gliding arc

Introduction

Plasma catalysis is an emerging technology, holding promise to improve existing technologies for a variety of applications, including air purification [1–5], hydrocarbon reforming [6–10], synthesis of nanomaterials [11–13], hydrogen production [14, 15], ammonia production [16, 17] and more. The advantages of plasma catalysis over traditional thermal catalysis are enabled by combining the high selectivity of the catalyst with the high reactivity of the plasma, as summarized in various reviews [2, 18–26]. In very general terms, the aim of plasma catalysis may be described as generating reactive species in the plasma and allowing them to react at the catalyst surface, forming the desired

✉ Erik C. Neyts
erik.neyts@uantwerpen.be

[1] Research Group PLASMANT, Department of Chemistry, University of Antwerp, Universiteitsplein 1, 2610 Wilrijk, Antwerp, Belgium

products with high conversion and very high selectivity, and at an energy cost as low as possible.

The underlying complexity of this seemingly simple concept, however, is overwhelming. Indeed, in spite of a significant number of studies in this field, little progress has so far been made regarding the fundamental processes taking place, enabling to steer the outcome. As a result, optimization of plasma catalysis setups, including e.g., reactor design, plasma process conditions and choice of catalyst, currently remains based on a trial-and-error approach, directed to a large extent by experience. This results in the wide variety in experimental setups encountered in the literature.

The envisaged opportunities for plasma catalysis are often considered to be due to the possible synergetic effects occurring when the plasma and catalyst interact. Synergy is here defined as the improvement in some process descriptor, such as selectivity, yield, or energy efficiency, as observed in the plasma catalytic process over the sum of the same descriptor in the thermal catalytic and pure plasma process.

There is a rich literature on such synergistic effects. Plasma/catalyst synergy in dry reforming of methane (DRM) was for instance demonstrated by Zhang et al. [27] using different Cu-Ni/γ-Al_2O_3 catalysts. It was found that the maximum CH_4 conversion in the plasma catalytic setup was 69 %, while it was only 13 and 10 % in the case of plasma-only conversion and thermal catalysis, respectively. Likewise, the CO_2 conversion amounted to 75 % in the case of plasma catalysis, to be compared with 2.5 and 13 % for plasma-only and thermal catalysis, respectively. Also the selectivities towards H_2 and CO were significantly better for plasma catalysis. It was argued that the origin of this spectacular process improvement was due to surface adsorption of reactive plasma species, followed by recombination of the adsorbed species. It was moreover suggested that the plasma may heat up the catalyst surface, thereby enhancing the desorption of surface species.

In the field of VOC abatement, Whitehead and Demidyuk found a decrease in activation barrier of more than 20 %, from 63.2 to 49 kJ/mol, for toluene decomposition on a Ag_2O/Al_2O_3 catalyst in a DBD plasma. In the case of a MnO_2/Al_2O_3 catalyst, an increase of more than 25 % in the pre-exponential Arrhenius factor was found. These effects were ascribed to the plasma-induced generation of oxygen radicals at the surface and a plasma-induced increase in surface active centers, respectively [28]. It should be realized, however, that the application of the Arrhenius equation is in principle restricted to thermal processes. While these experiments therefore quite clearly demonstrate a qualitative effect, it is not clear to what extent their quantitative interpretation can be justified.

While these examples indicate quite clearly that important synergistic effects may take place when combining the plasma with a catalyst, such synergy is by no means always observed, and the combination of catalyst and plasma has in some cases even been described to adversely affect the process [29, 30]. Moreover, plasma catalysis also suffers from a number of drawbacks and challenges compared to thermal catalysis and plasma-only processing, including e.g. the additional energy cost for initiating and maintaining the plasma or the efficient integration of the catalyst in the discharge chamber, respectively.

For instance, In the field of hydrocarbon reforming, the reported energy efficiencies currently remain significantly below the thresholds required for commercial application. Plasma catalysis is currently nowhere near to competing with steam reforming of methane for hydrogen production or for synthesis of synthetic fuels. Specifically, the highest reported energy efficiency for dry reforming of methane is 60 % for a conversion of 8–16 % [31], to be compared to 85 % energy efficiency for a conversion of about 60 % for steam reforming of methane. With respect to the integration of the catalyst in the discharge volume, it has been found that this may either result in a positive or a negative effect. For

instance, Tu et al. [32] found that upon partially filling the plasma reactor with dielectric beads or catalyst coated pellets, the typical discharge mode is the formation of filamentary microdischarges whereas fully packing the reactor volume resulted in the formation of surface discharges [33], which in turn leads to a decrease in CH_4 and CO_2 conversion in plasma catalytic DRM.

A more fundamental understanding of the process is likely to significantly advance the field. In this review, the various factors coming into play in plasma catalysis processing shall be discussed, viz. neutrals (including molecules, radicals, metastables and atoms), ions, electrons, photons and electric fields, and how these factors determine the occurring plasma—catalyst surface interactions, viz. adsorption, desorption, surface chemical reactions, photocatalyst activation, surface modification, heating, charging, surface discharge formation and electric field enhancement. While of great importance, a discussion of the effects of nanoscale catalyst features on the plasma catalytic process, including e.g. nanoscale thermodynamics, non-equilibrium thermodynamics, the size-dependent adsorption energy of reactive species on nanocatalysts, the Gibbs–Thomson effect, etc., is outside the scope of the current review. A recent review on the importance of some of these nanoscale effects on the thermodynamics of plasma catalysis, however, can be found in [34], while discussions on specific nanocatalyst properties in general can be found in e.g. [35]. Here, the focus shall be instead on the individual elementary processes and their dynamics.

Plasma Sources in Plasma Catalysis

In a plasma catalytic setup, the catalyst may be combined with the plasma in two ways. The catalyst may be integrated directly into the plasma zone, in which case it is called single-stage plasma catalysis, or the catalyst and the plasma zone may be located in spatially different areas, in which case the process is termed two-stage plasma catalysis. The factors contributing to the plasma catalytic process in a two-stage setup include long-lived radicals, neutrals and possibly metastables, i.e., those species which have a sufficient life-time to be transferred from the plasma zone to the catalyst zone. Hence, in this case, the role of the plasma is limited to modifying the composition of the gas prior to interaction with the catalyst. The factors contributing to the plasma catalytic process in a single-stage setup are not or to a much lesser extent limited by their life-time, and hence also include highly reactive radicals, ions, electrons, and photons, in addition to the aforementioned long-lived species. Moreover, in a single-stage setup, also an electric field may be present at and near the catalyst surface.

What eventually interacts with the surface, is entirely determined by the type of plasma and the plasma conditions. Experimentally, various discharge types are used for plasma catalysis, including dielectric barrier discharges (DBDs), gliding arcs, plasma jets and corona discharges. Here, two representative and very different types of plasmas used plasma catalysis will first be shortly discussed: single-stage atmospheric pressure dielectric barrier discharges, and two-stage atmospheric pressure gliding arcs.

Dielectric Barrier Discharge

The most often used type of discharge in plasma catalysis is the (atmospheric pressure) dielectric barrier discharge (DBD). A DBD usually consists of two electrodes of which at

least one is covered with a dielectric layer. The discharge is formed in the gap between the electrodes, which are typically arranged in a planar or cylindrical configuration. Two typical setups, corresponding to single-stage and two-stage plasma catalysis, are shown in Fig. 1 [36]. Gas breakdown is initiated through a large number of independent microdischarges, called filaments [37, 38]. The function of the dielectric barrier is to prevent the formation of an arc discharge, and to limit the amount of charge accumulating on the surface. DBD's are strongly non-uniform plasmas, and allow ionization very close to the surface due to the continuous formation of microdischarges. These microdischarges develop quickly and last for a few nanoseconds to several tens of nanoseconds, before extinguishing due to limited current flow. This, in turn, causes significant charge build up at the dielectric surface. Every time the polarity of the field changes, a new filament is created at the location of the charge spot. The gas in between the filaments is mostly not ionized, although photo-ionization and diffusion of charged particles may lead to some degree of ionization.

In the case of plasma catalysis, the operating temperature is usually rather low, in the order of 500–700 K. Note, however, that the local surface or catalyst temperature might (temporarily) be higher, considering the very nature of the microdischarges. The ion density will typically be low, since the ionization degree decreases as the square of the pressure [39]:

$$\frac{n_e}{n_0} \propto \frac{1}{p^2} \tag{1}$$

where n_e is the electron (or ion) density and n_0 is the gas density. The resulting ionization degree is in the order of 10^{-4} [40] such that in the filaments, an electron density of 10^{14}–10^{15} cm^{-3} and a current density of 10^2–10^3 A cm^{-2} is typically reached [36]. Moreover, the collisional nature of the sheaths leads to ion energy distributions shifted towards low energies, and hence surface damage induced by energetic ions is largely prevented in atmospheric plasmas [41].

At the contact point of the microdischarge and the surface, the filament spreads out. The typical filament diameter is in the order of 100 μm, which is much larger than the typical

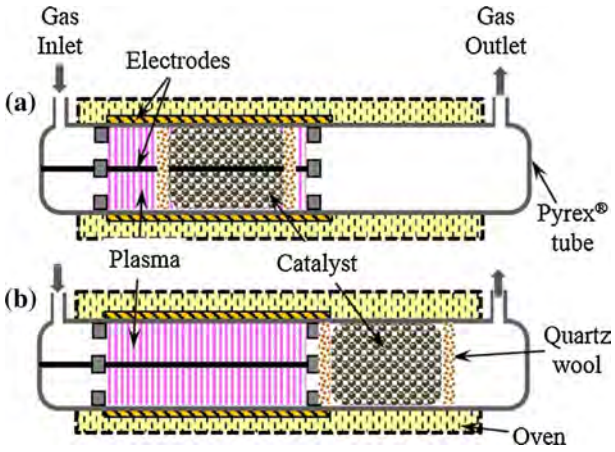

Fig. 1 Typical **a** single-stage and **b** two-stage dielectric barrier discharge setup used in plasma catalysis. Reproduced with permission from [36]

sizes of nanofeatures or nanocatalyst particles dispersed on the substrate material. A model for a single microdischarge is shown in Fig. 2. The charge transported by a filament is in the order of 100 pC, while the energy is in the order of μJ. Therefore, these filaments will normally hardly heat up the surrounding gas, but they may heat up the local surface, at least temporarily.

The photon flux delivered to the surface by impinging streamers in filamentary DBDs was calculated by Babaeva to be in the order of 10^{22} cm^{-2} s^{-1}, to be compared with ion fluxes which are generally several orders of magnitude lower, in the order of 10^{19}–10^{20} cm^{-2} s^{-1} [42].

In the context of plasma catalysis, the reactor volume is often filled or partially filled with pellets or beads of dielectric material, resulting in a so-called packed bed discharge. In this case, the plasma is created between the pellets. Depending on the pellet properties such as dielectric constant, size and surface morphology, the electric field can be significantly enhanced near their surface, by a factor of 10–250 [43]. This effect will be discussed further in Sect. 3.8. These pellets can also be coated with catalytic material, ensuring a large accessible catalyst surface in contact with a high electric field.

Gliding Arc

A gliding arc discharge (GAD) is a so-called transitional discharge or warm plasma, indicating that it is neither a non-thermal plasma (characterized by a gas and ion temperature of several hundred Kelvin and an electron temperature of several eV), nor a thermal plasma (characterized by a more or less uniform temperature for all species, typically 10,000 K or above). Gliding arcs are instead characterized by a relatively high gas temperature of 1000–3000 K, but still maintain non-equilibrium between electrons and heavy particles [43, 44]. A gliding arc is created by the initiation of an arc between two diverging electrodes at their smallest separation. Due to the gas flow, the arc gradually moves down the electrodes until it extinguishes at the end to the electrodes. A new arc is then initiated. The arc in the GAD goes through three sequential stages, viz. breakdown, equilibrium stage and non-equilibrium stage. The typical setup of the gliding arc and the

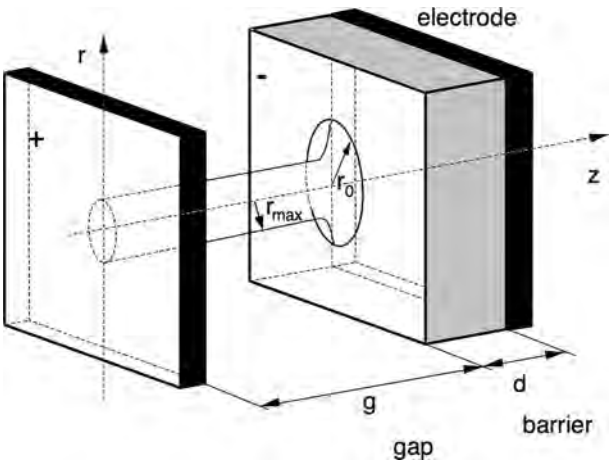

Fig. 2 Structure of a single microdischarge in a DBD. Reproduced with permission from [38]

three stages are schematically represented in Fig. 3. It is the non-equilibrium stage which is most important for plasma catalysis. Indeed, the simplest setup is a two-stage setup, where the catalyst is placed downstream from the discharge [45]. In principle, however, the catalyst material can also be incorporated through dispersion directly in the gas flow [46]. Typically, the gliding arc works at atmospheric pressure. The electron temperature in the non-equilibrium stage is about 1 eV [47]. An important advantage of gliding arcs over e.g. DBDs is their high throughput, in the order of liters to tens of liters per minute [48].

Elementary Plasma-Surface Interaction Processes in Plasma Catalysis

The interaction between a plasma and a catalyst is a highly complex phenomenon comprising a large number of elementary processes. These processes will be described below.

Adsorption

The key process in heterogeneous catalysis is the surface chemical reaction. The catalytic conversion of reactants into products can be separated into three steps, viz. adsorption of the reactants, the surface chemical reactions and desorption of the product molecules. In plasma catalysis, the adsorption of neutral molecules as occurs in thermal catalysis is supplemented by adsorption of atoms, radicals, ions and electrons at the surface.

Adsorption of Neutral Species

Adsorption is one of the key elementary processes in any heterogeneous catalytic process, including plasma catalysis. Adsorption is the primary process enabling molecules to be transformed at the surface by post-adsorption chemical reactions, and may proceed through physisorption or chemisorption, depending on the nature of the adsorption interactions.

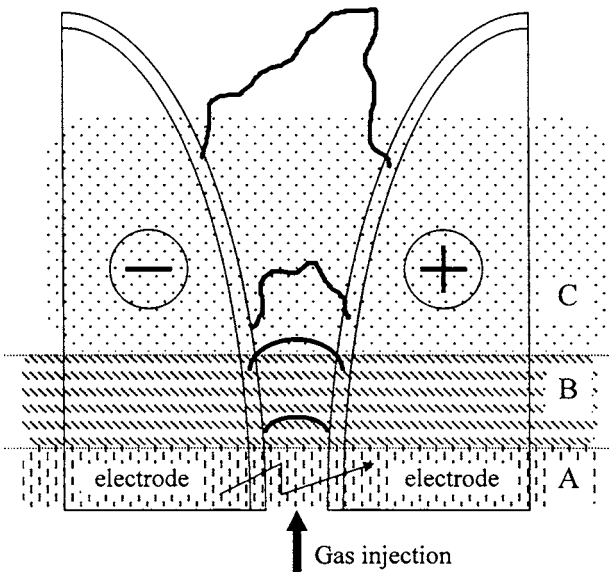

Fig. 3 Typical gliding arc setup, showing the three stages of gliding arc evolution: (*A*) reagent gas breakdown; (*B*) equilibrium heating phase; and (*C*) non-equilibrium reaction phase. Reproduced with permission from [47]

Note, however, that the distinction between physisorption and chemisorption is ill-defined, yet remains in use because of its historical and intuitive nature.

In the framework of classifying types of adsorption, physisorption may be defined as the non-permanent and non-specific attachment of molecules to a surface through dipole and dispersion interactions. Depending on the local surface properties and the adsorbent polarity, these interactions may consist of dipole–dipole (Keesom) type or dipole—induced dipole (Debye) type, in addition to London dispersion forces. Physisorption energies are typically low compared to the much stronger chemisorption energies, in the order of 10–100 meV, although dipole–dipole interactions can in some cases be much stronger and even become comparable to typical chemical bond energies, up to $\sim$1.5 eV.

There is no barrier for molecules approaching the surface to enter the physisorption well, and the process is hence not activated. This is important for plasma catalysis, as heating the substrate is typically avoided or at least lowered compared to thermal catalysis, in order to reduce the energy cost. Since physisorbed species are not strongly bound to the surface, they can easily diffuse over the surface, so as to "find" a surface species to react with. Physisorption thus also significantly increases the life time of the reactant near or at the surface, compared to pure impact and reflection. This increased life time is considered to be crucial in e.g. plasma catalytic VOC abatement, where the species to be processed are typically present in low concentrations. The surface captures the VOC molecules, allowing oxidizing molecules from the plasma phase to initiate their destruction [25].

Chemisorption is the adsorption of atoms, radicals or molecules at a surface through the formation of chemical bonds. Consequently, the adsorption strength is much larger compared to physisorption, typically in the order of several eV per bond, and the adsorbed molecules are much less mobile. In the context of plasma catalysis, the interaction of adsorbate species with traditional catalyst transition metals is of special interest, and shall be considered here. When an atom or a radical approaches the surface, its valence states may directly couple with the metal catalyst *s*- and *d*-bands. While the interaction with the *s*-bands is very similar for all transition metals, the catalytic characteristics are mainly determined by the metal *d*-states. Generally speaking, the higher the energy of the *d*-band (i.e., going from left to right in the periodic table), the more antibonding states will lie above the Fermi level and hence the stronger the bond. Thus, Cu generally shows a weaker adsorption of atoms and molecules, while Ni or Fe form stronger bonds. Consequently, Cu is generally less reactive and Fe and Ni are more reactive. A thorough description of the bonding process and electronic nature of the interaction can be found in [49, 50].

Energetically, sticking of an incoming particle requires (partial) dissipation of its kinetic energy into other degrees of freedom [51]. This energy may be dissipated in one or several of five channels. Usually, some of the kinetic energy is dissipated in the excitation of surface phonons, which in turn are further dissipated in the bulk substrate. Thus, the catalyst then acts as a semi-infinite heat bath, thermalizing the incoming particle. This mechanism is of particular importance in case there is no significant difference in electronegativity between adsorbate and surface atoms. Alternatively, energy may also be dissipated in the (non-adiabatic) excitation of electron–hole pairs, leading to the formation of a hot electron (with energy above the Fermi level) and a hot hole (with energy below the Fermi level). This mechanism is important when the difference between the electronegativity of adsorbate and surface atoms is significant. Part of the kinetic energy of the impinging particle may also be dissipated in lateral motion of the particle, especially if the surface is corrugated. Thus, in this case the relaxation of the momentum component normal to the surface will relax much faster than the tangential components. Species showing such behaviour are termed hot precursors or intrinsic precursor species [52]. This is very

important in plasma catalysis, as the surface area of the catalyst is typically maximized by maximizing the catalyst dispersion, and surface features are typically in the nanometer length scale. Further, in the case of molecules, the initial kinetic energy may be coupled to internal degrees of freedom upon impact, i.e., excitation of the vibrational and rotational degrees of freedom. Depending on how this energy is redistributed over those internal degrees of freedom, this energy dissipation process determines the subsequent surface processes. Finally, the molecule may also dissipate energy by dissociation. Most chemisorption processes of molecules are dissociative. Very often, dissociative chemisorption is the rate limiting step of a catalytic process.

Adsorption of Charge Carriers and Surface Charging

The key difference between the plasma state and the gaseous state is the presence of free electrons and ions, i.e., free charges. Charges are naturally expected to play a critical role in plasma catalysis as well, since catalysis is to a large extent controlled by bond breaking and bond formation processes, which in turn are determined by the flow of electrons and the diplacement of the atoms or molecular fragments involved. Yet, very little attention is generally paid to charge transfer processes in the plasma catalysis literature.

Every floating surface in contact with a plasma will usually acquire a negative charge, due to the much higher mobility of the electrons compared to the ions. Thus, such surfaces are usually covered by a quasi-stationary electron film. A model describing the formation of this film was put forward by Bronold et al. Based on this model, a surprisingly low electron sticking coefficient $s = 10^{-4}$ and an equally surprising long life time $\tau = 10^{-2}$ s were obtained for a metal surface [53]. Turning to dielectric surfaces, dedicated experiments on charge trapping were carried out by Ambrico et al. [54, 55] on alumina in a DBD setup in different gas mixtures and discharge modes. It was found that plasma electrons are effectively trapped at the alumina surface. The trapped electrons were found to have a relatively low energy of 1 eV. Due to their low energy, the electron penetration depth was only a few nanometers. These generated charge traps are long-lived, with a life time up to several days. A marked difference was observed for different discharge modes. The density of trapped surface charge was found to be significantly higher for the DBD in glow discharge mode compared to filamentary mode.

This phenomenon of surface charge trapping has important consequences for the formation of streamer initiation and propagation [56]. Specifically, Guaitella et al. [56] demonstrated that photons emitted by an single filament cause photo-desorption of trapped surface charges, leading to the collective initiation of large current peaks. This collective effect was further found to be enhanced in the presence of a porous photocatalytic TiO_2 surface. I contrast, both external UV radiation and the presence of adsorbed C_2H_2 were found to diminish the collective effect.

Ions are not expected to play a major role, due to their typically low energies in atmospheric plasmas as usually applied in plasma catalysis. Nevertheless, the ion distribution will also contain a (small) fraction of rather energetic ions, and these may potentially influence the surface morphology, and thereby the catalytic properties of the surface. This will be described in Sect. 3.5.

Surface Chemistry

Surface chemistry is the very heart of catalysis and plasma catalysis. Provided that efficient mechanisms for delivery and removal of molecules to the surface are in place, it is the

nature of the various reactions occurring at the catalyst surface which eventually determine the activity, selectivity, and energy efficiency of the overall process. In turn, the dynamics of the elementary processes involved are determined by the energy exchange between the catalyst support and the catalyst surface on the one hand, and the catalyst surface and the various modes of the reactants on the other hand. The time scale associated with this energy exchange then determines how these dynamics may be appropriately described. In general, we can distinguish thermal surface processes from non-thermal processes. In the former case, the prerequisite is that the relaxation time to thermal equilibrium is much shorter than the atomic motion of the atoms involved in the reaction. Processes fulfilling this requirement will be discussed in the next section (Sect. 3.2.1). Surface reactions which—as a rule of thumb—occur on subpicosecond time scales, however, cannot be considered as thermal reactions, and will be discussed in Sect. 3.2.2.

Thermal Surface Chemistry

The three prototypical thermal surface reaction mechanisms, i.e., the Langmuir–Hinshelwood, Eley–Rideal and Mars—Van Krevelen mechanisms, are depicted schematically in Fig. 4 [57].

Langmuir–Hinshelwood Mechanism The classical description of surface reactions in heterogeneous catalysis is through the Langmuir–Hinshelwood mechanism. In this mechanism, the reaction between two species proceeds starting from both molecules in the adsorbed state, equilibrated with the surface. Typically, the Langmuir–Hinshelwood mechanism is considered to occur if the time between reactant adsorption and product formation exceeds the time scale required for thermalization, i.e., in the order of about 10 ps.

The kinetics associated with this mechanism is appropriately called Langmuir–Hinshelwood (LH) kinetics. In LH kinetics, the rate r of the reaction between two species A and B on the surface S is given by

$$r = k\theta_A\theta_B \tag{2}$$

where k is the rate constant for the overall reaction, and θ_A and θ_B represent the surface coverage by molecules A and B, respectively. The surface coverages can be related to the partial pressures of the molecules through the Langmuir isotherm, such that

$$r = k\frac{K_A p_A \cdot K_B p_B}{(1 + K_A p_A + K_B p_B)^2} \tag{3}$$

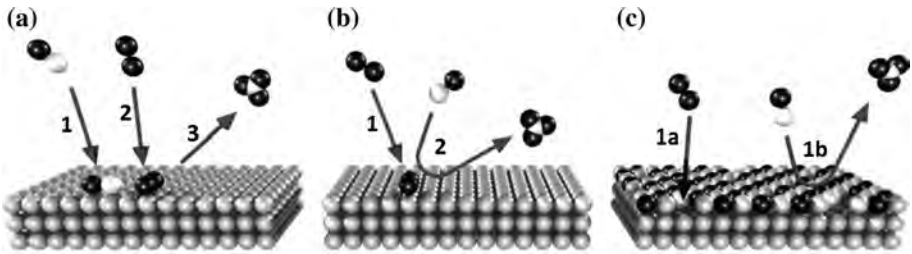

Fig. 4 The three prototypical thermal surface reaction mechanisms, **a** Langmuir–Hinshelwood; **b** Eley–Rideal; and **c** Mars—Van Krevelen. Reproduced with permission from [57]

where K_A and K_B are the equilibrium constants for surface adsorption of molecules A and B, respectively, and p_A and p_B are the corresponding partial pressures.

The LH model is a limiting case and an idealized description of the true process, based on a number of approximations. Molecules are considered to be hard-spheres, and are assumed to be in thermal equilibrium with the surface. The surface coverage is assumed to be constant and reside in a steady state. The reaction between the molecules is assumed to be the reaction rate limiting step, and to be independent of mutual interactions prior to the reaction, i.e., the probability of an incoming molecule to adsorb on any particular site is independent of the occupation of nearby sites. Also, the molecules are assumed to be randomly distributed over the surface, where each molecules occupies precisely 1 surface site. All surface sites are moreover considered to be equivalent.

While most of these assumptions may indeed be valid to a certain extent under high vacuum conditions on perfectly crystalline surfaces, the situation is obviously much more complicated in plasma catalysis at atmospheric pressure, making use on nanofeatured catalysts with instrinsic roughness. Hence, while some researchers have invoked Langmuir–Hinshelwood kinetics to explain experimental observations [58, 59], such analysis must be treated with caution.

Eley–Rideal Mechanism The second, often invoked mechanism in catalysis is the Eley–Rideal (ER) mechanism. In this case, a pre-adsorbed surface species in thermal equilibrium with the surface is assumed to react with an incoming gas-phase particle. The resulting product molecule subsequently desorbs from the surface. Again, the actual reaction is assumed to be the rate limiting step. The rate for the ER mechanism is given by

$$r = k\theta_A p_B \tag{4}$$

where p_B is the partial pressure of species B. An example relevant for plasma catalysis is the formation of CH_4 from association of an impinging H-atom and an surface-adsorbed $CH_{3,ads}$ species on a Cu(111) surface [60].

However, while the ER mechanism seems reasonable, it turns out that only very few reactions truly operate according to this mechanism in its pure form [52]. Instead, it seems that many surface reactions proceed through closely related processes in which the incoming species are partially accommodated at the surface, and which should hence rather be classified as hot precursor processes (see below).

Mars and Van Krevelen Mechanism The Mars and Van Krevelen (MvK) mechanism is characterized by the incorporation of one or more lattice consistituents of the catalyst into the product molecules [61]. The catalyst is subsequently replenished through adsorption and uptake of corresponding species from the gas (or plasma) phase. Hence, in this case, the catalyst is temporarily consumed. While mostly applicable to oxides, reactions on sulfides, chlorides or hydrides may proceed along the same mechanism. Although all MvK processes are redox reactions, it is incorrect to state that all heterogeneous catalytic redox reactions on metal oxide surfaces proceed through the MvK mechanism, and hence the alternative terminology "redox mechanism" should be avoided. Moreover, it was claimed that the original rate expression for this mechanism is inconsistent and erroneous [62], and LH-type rate expressions provide an equal or even better description.

Non-thermal Surface Chemistry

Precursor Molecules with Internal or Kinetic Energy In the framework of thermal surface reactions, adsorbing molecules are considered to first thermalize with the surface before dissociating or reacting with co-adsorbed species, implying a redistribution of energy upon impact over the various available degrees of freedom. In case of the presence of an activation barrier for the reaction, as is most often encountered, it is in principle more efficient if this redistribution does not occur, but instead an accumulation of energy occurs in one or several specific degrees of freedom. This typically either translational kinetic energy or vibrational energy of the impinging molecule. In Fig. 5, the corresponding mechanisms are schematically depicted for dissociative chemisorption and molecular physisorption of methane [63]. In panel (A), methane approaches the surface with energy greater than the effective reaction barrier, leading to dissociative chemisorption. In panel (B1), methane approaches the surface with insufficient energy to surmount the energy barrier, and becomes trapped in a molecular physisorbed state, until it escapes to the chemisorption well with rate constant k_c or desorbs with rate constant k_d, as shown in panel (B2). In panel (C1), a vibrationally excited methane molecule approaches the surface and becomes trapped in the physisorbed state, until it enters the chemisorption state with rate constant k_c or desorbs with rate constant k_d, as shown in panel (C2). In comparison to the case depicted in panel (B2), however, the relative rate for chemisorption is increased due to the additional internal energy of the molecule. In the case of desorption, the molecule may either leave the surface in the vibrational ground state if vibrational quenching takes place, or it may desorb in an excited vibrational state.

A typical example is the dissociative chemisorption of methane on the Ni(111) surface. As shown in Fig. 6, the dissociation probability of CH_4 (and CD_4) increases exponentially with the normal component of the translational energy of the impinging molecule [64, 65].

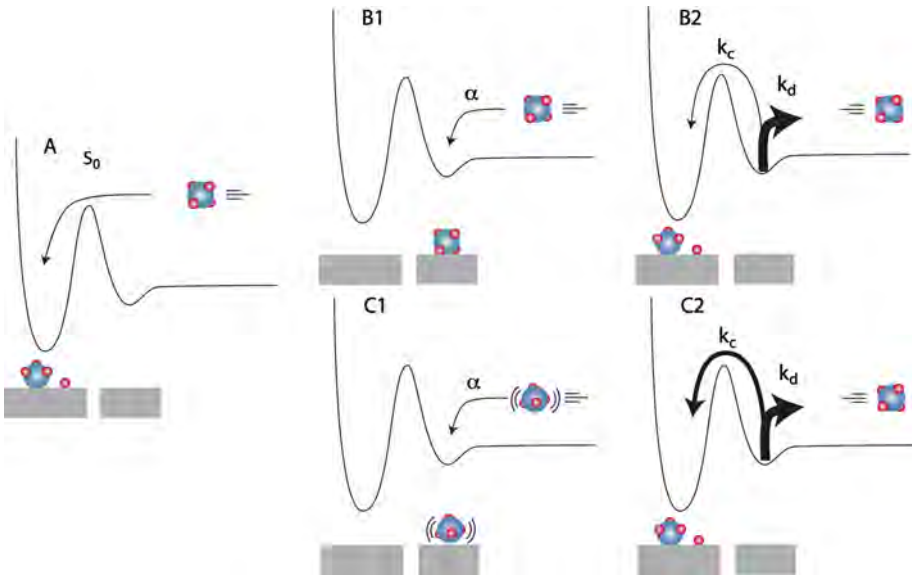

Fig. 5 Schematic representation of possible reaction mechanisms in methane adsorption. Reproduced with permission from [63]

These experiments also demonstrated that the surface temperature was of no influence. It is believed that the effect of the translational energy is to deform the methane molecule upon impact in a pyramidal configuration, allowing three hydrogen atoms to interact at the same time with the surface [52].

Vibrational excitation of a molecule may also enhance its surface reactivity, through lowering of the effective activation barrier. This may occur in two ways [66]. First, the vibrational energy increases the energy level of the reactant. Relative to the barrier with respect to the vibrational ground state, the effective barrier is thus lowered. Second, also the energy of the transition state may be lowered, since the vibrationally excited molecule may have access to part of phase space which is inaccessible to the ground state molecule, and thus have access to an alternative minimum energy path.

However, not every vibrational mode will give rise to the same increase in reactivity upon excitation. For instance, Juurlink et al. [67] investigated dissociative chemisorption of CH_4 on Ni(111), and found for instance that the $3\nu_4$ is significantly less effective than the ν_3 C–H stretch at promoting dissociative chemisorption, even though $3\nu_4$ contains 30 % more energy. This result therefore provides clear evidence for vibrational mode specificity in a gas-surface reaction.

Collision-Induced Surface Reactions In collision-induced surface reactions, the energy required to overcome the surface reaction energy barrier is delivered by an incoming particle, which is otherwise not involved in the chemical reaction itself. For instance, Beckerle et al. [68, 69] studied the dissociation of pre-adsorbed CH_4 molecules on a

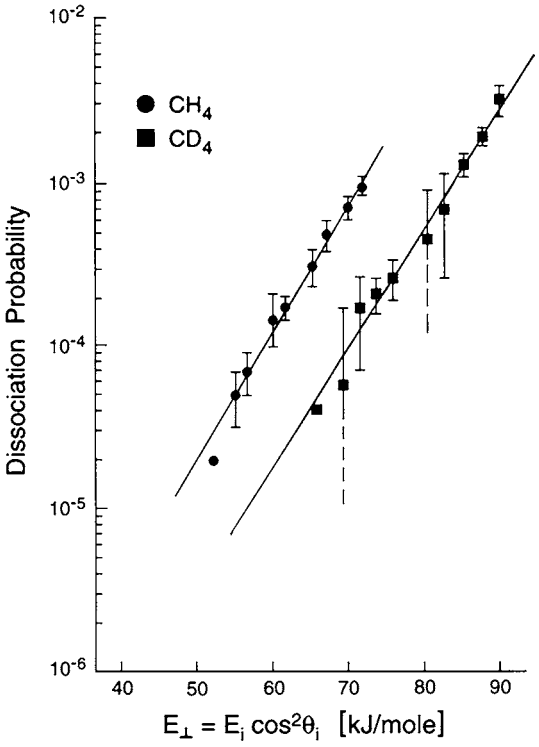

Fig. 6 Measured dissociation probabilities of CH_4 and CD_4 impinging onto a Ni(111) surface as a function of the normal component of translational energy. Reproduced with permission from [64, 65]

Ni(111) surface by energetic Ar atom impacts. The mechanism may conceptually be understood to occur in two consecutive steps. First, the impinging Ar atom transfers part of its energy to the adsorbed CH_4 molecule. The fraction of energy transferred depends on the angle and point of impact. Subsequently, the energy accumulated in the direction normal to the surface may be used to decompose the molecule in the same way as would occur if the CH_4 molecule would impinge with sufficient kinetic energy on the surface, as described above in Sect. 3.2.2.1.

Collision induced surface processes are also pertinent to chemisorbed systems, provided the impinging particles have sufficient energy to overcome the relevant dissociation and/or desorption barriers. For instance, collision-induced O_2 dissociation and desorption following Xe impacts on a coadsorbed CO + O_2 adlayer was demonstrated by Åkerlund et al. [70] on the Pt(111) surface. Moreover, also CO_2 formation was observed Similarly, Vattuone et al. [71] demonstrated Xe-collision induced O_2 dissociation and desorption from a Ag(001) surface. Interestingly, the branching ratio between dissociation and desorption was found to be a function of the impinging gas atom energy and angle of incidence, the latter being attributed to surface corrugation.

Hot Precursor Surface Reactions Hot precursor species are species which are trapped at the surface, but which have not yet attained thermal equilibrium with the surface. This occurs when upon hitting the surface, the velocity component of the particle normal to the surface quickly decreases to near-zero, while the lateral components do not. The particle can then travel over substantial distances over the surface before attaining thermal equilibrium, since the barriers for surface diffusion are typically much lower than escape from the chemisorption well.

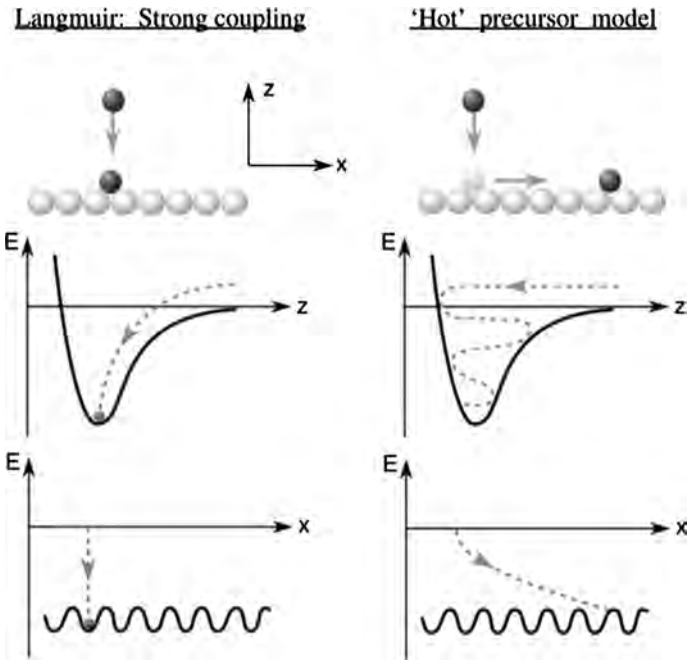

Fig. 7 Schematic dynamics for adsorption following (*left panel*) the Langmuir concept or strong coupling limit, and (*right panel*) the hot precursor model. Reproduced with permission from [52]

This process can be understood in terms of the model put forward by Ertl [52], depicted in Fig. 7. In the strong coupling limit, the particle immediately attains thermal equilibrium with the surface upon sticking, and typically transfers its energy to the surface through direct phonon excitations. In the hot precursor model, in contrast, the particle initially couples only weakly with the surface, and first hits the repulsive wall of the surface. The energy of the particle is then transferred stepwise to the surface.

Alternatively, hot surface species may also be formed through exothermic surface reactions. The heat released during an exothermic reaction will usually be transferred most efficiently to the surface, but part of this energy may also be transferred to the reaction products. This energy may then be used either to allow the products to diffuse over the surface, or even to desorb from the surface.

Experiments demonstrating the existence of this hot precursor model are normally carried out at low temperatures, to reduce the influence of thermal diffusion and other thermal processes. However, even at typical plasma catalysis processing temperatures, the energies involved will generally be higher than the thermal energy, and may hence have an important effect and contribute to the overall process.

Photon-Induced Surface Reactions Impinging photons may induce surface reactions either through heating the electrons in the solid, or by single photon absorption, provided that the photons have sufficient energy. Heating the electron gas leads to partial occupation of an adsorbate antibonding level, triggering the surface reaction. An example of this process is the associative desorption of CO_2 from co-adsorbed CO and O on a Ru(0001) surface, induced by femtosecond infrared laser pulses [72]. The desorption of NH_3 from a Cu surface, on the other hand, was shown to be initiated by single photon absorption [73]. In this case, the primary excitation is the creation of a hot electron, which is captured by the adsorbate NH_3 molecule. This in turn causes a Franck–Condon transition from the ground state to a repulsive excited state, which induces the desorption process.

Desorption

Together with adsorption and surface chemical reactions, desorption of product molecules from the catalyst surface is an essential process in plasma catalysis. The kinetics of the thermal desorption process may be described by the following rate law:

$$r = k_{des}\theta^n \tag{5}$$

where θ is the surface concentration of adsorption species, and n is the kinetic order. Atomic or unimolecular desorption is usually first order, while recombinative molecular desorption (as e.g. occurs after a Langmuir–Hinshelwood surface reaction) is usually a second order process. Sometimes the term surface film reaction (SFR) is used to denote the latter process. In the case of thermal desorption, the rate constant k_{des} is usually described by a simple Arrhenius equation

$$k_{des} = A\exp\left(\frac{-E_a^{des}}{RT}\right) \tag{6}$$

where A is the so-called pre-exponential factor, often identified with an escape attempt frequency, E_a^{des} is the activation barrier for desorption, often identified with the enthalpy of adsorption, R is the universal gas constant and T is the surface temperature. In this case, the resulting rate expression is referred to as the Polanyi-Wigner relation [74].

Note, however, that desorption may also occur as the result of an electronic exitation, as described above in Sect. 3.2.2.4, or through sputtering or etching, as described in Sects. 3.5.3 and 3.5.4

Photocatalyst Activation

Photons

Since plasmas are sources of UV radiation, the use of photocatalysts has been considered for, e.g., CO_2 reduction and VOC abatement [25, 75, 76]. In principle, any energy source capable of exciting an electron from the valence band to the conduction band of the photocatalyst can be used. Clearly, however, photons are most efficient to induce this process, and this is hence by far the most common route for photocatalyst activation. Essentially, the activation process consists of the formation of an electron–hole pair. In light-induced electron–hole pair generation, photons carrying an energy equal to or larger than the band gap are absorbed by the photocatalyst. An electron is then excited from the valence band to the conduction band, while the hole is left behind in the valence band. Photocatalysis then relies on the excited electron to reduce the source molecule to the targetted species, while the hole oxidizes another molecule (e.g. H_2O). This process is schematically depicted in Fig. 8 [77].

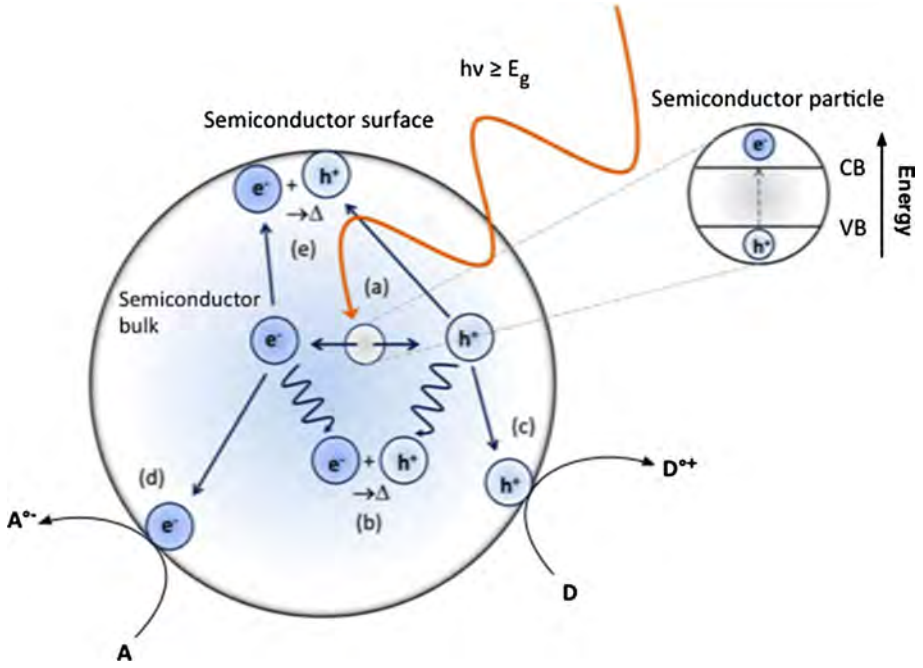

Fig. 8 Photo-excitation of a semiconducting metal oxide particle (*a*) and the de-excitation events; (*b*) electron–hole recombination within the semiconductor bulk, (*c*) oxidation of surface adsorbed electron donors, (*d*) reduction of surface adsorbed electron acceptors and (*e*) electron–hole recombination at the semiconductor surface. Reproduced with permission from [77]

The possibility and efficiency of photocatalyst activation by plasma photons is not yet resolved. There have been claims that the plasma can indeed produce enough and sufficiently energetic photons to induce photocatalytic surface reactions, e.g., for the abatement of VOC's [75, 78, 79]. While these studies have indeed shown an increase in VOC destruction upon application of the plasma in the presence of a photocatalyst, it was not unambiguously demonstrated that this was due to plasma-induced photocatalytic reactions. In contrast, it has also been claimed that typical plasma sources used in plasma catalysis do not create a sufficient photon flux to generate an appreciable effect [22, 80–82]. More research is needed to elucidate this issue further.

Particles

In principle, particles may also induce the generation of electron–hole pairs in the photocatalyst. These particles include electrons, ions and metastables. Note, however, that in this case the electron–hole pair generation involves a Coulomb interaction, which is intrinsically different from the photoelectric effect that is responsible for light-induced photocatalyst activation, and both of these are intrinsically different from the phonon-induced electron–hole pair generation discussed below in Sect. 3.4.3.

In the case of particle-induced electron–hole pair creation, the impinging particle carries sufficient energy to knock-off a valence electron from an atom. The energy released in this process may be used to excite the knock-off electron to be excited to the conduction band. Although Mei et al. [10] claim electron-induced photocatalyst activation to occur in their packed bed DBD reactor, there are to date no reports in the literature actually demonstrating such a process in the context of plasma catalysis.

Electron-induced CO_2 dissociation was observed e.g. on rutile TiO_2 (110) surfaces [83, 84]. This process, however, was governed by a direct electron injection into the CO_2 LUMO orbital, and can hence not be catagorized as an electron-mediated photocatalyst activation process. Indeed, the observed CO_2 reduction process may not happen by photo-generated electrons, since the photo-generated electrons may rapidly thermalize to the conduction band edge, which is much lower than the reduction potential of the CO_2/CO_2^{*-} couple [85].

Thermal Fluctuations

Finally, also thermal fluctuations may induce carrier generation. In this case, an electron from the valence band absorbs lattice phonons to be excited to the conduction band. Note, however, that since the phonon energy is typically much lower than the band gap, excitation to the conduction band can only happen through a multiphonon process. In this case, the electron is first excited to a trap level in the band gap, and subsequently absorbs another phonon to reach the conduction band.

Surface Modification

Upon interaction with the surface, the plasma modifies the surface structure through a number of processes. These processes are described below, and depicted schematically in Fig. 9.

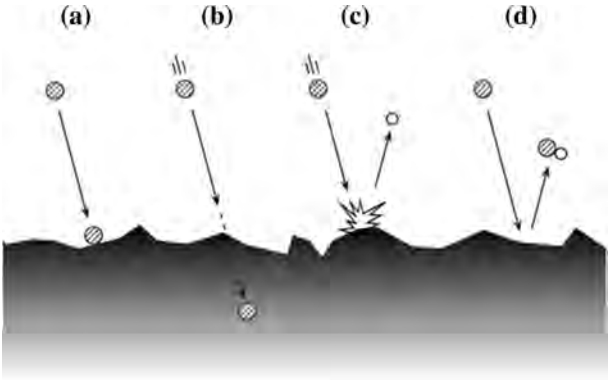

Fig. 9 Schematic representation of several surface modification processes. (*a*) Poisoning by strong adsorption and blocking active catalytic sites; (*b*) implantation of the highly energetic impinging particle in the bulk of the substrate; (*c*) sputtering by energetic ion impact; and (*d*) etching, through the formation of a volatile compound

Dissolution and Poisoning of the Catalyst

A critical issue in any catalytic process is to keep the catalyst active during operation. Poisoning of the catalyst, rendering the catalyst inactive, can occur either by irreversible surface adsorption of strongly binding species, preventing them to desorb and thereby blocking active catalyst sites (Fig. 9a), or by dissolution of atoms in the catalyst, modifying the catalytic properties, through changes in the geometrical, morphological or electronic structure of the catalyst, which is generally undesirable.

A typical example is the dry reforming of methane on Ni-surfaces. In this process, atomic carbon is formed, dissolving into the catalyst, and eventually covering the catalyst surface with amorphous carbon material [86, 87]. This process is referred to as coking. The deposited carbon is strongly bound to the surface, and prevents the adsorption of newly impinging molecules on the surface, thereby making the catalyst surface inactive.

Importantly, however, it has also been demonstrated that plasmas may effectively regenerate poisoned catalysts. For instance, Kim et al. [88] demonstrated packed-bed plasma regeneration of a Au/TiO_2 catalyst deactivated by the adsorption of VOCs, Sivachandrian et al. [89] studied regeneration of a isopropanol saturated TiO_2 surface, also in a packed-bed reactor, and Mok et al. [90] compared thermal and plasma regeneration of a desactivated Ni/alumina catalyst, to name but a few. The global operative mechanism appears to be the oxidation of the surface-adsorbed species, while the microscopic mechanisms naturally depend on the exact species and surfaces involved.

Implantation

In principle, energetic ions can penetrate the catalyst surface, and become implanted in the bulk of the catalyst (Fig. 9b). This again modifies the morphological and electronic structure of the catalyst, possibly altering its activity, stability, selectivity and other properties. In the context of catalysis, implantation has for instance been used for graphene synthesis on Ni thin films [91]. Implantation, however, typically requires keV ion energies. Considering that such high ion energies in plasma catalysis are highly unlikely due to the

collisional nature of the discharges employed, it is very unlikely that implantation plays an important role.

Sputtering

In contrast to implantation, sputtering only requires energies equal to or larger than the binding energy of surface atoms or molecules. Sputtering is schematically represented in Fig. 9c. Since surface atoms are undercoordinated, their binding energy is much lower than the bulk binding energies, and hence sputtering typically requires relatively low threshold energies. The sputter yield generally depends on various factors, including the type of surface, the impacting particles, their angle of incidence and their kinetic energy [92]. The thresheld energy is typically in the order of 10 eV. In the context of plasma catalysis, however, this energy is already relatively high, and only a very small fraction of the ions will have such an energy. Given that the yield at the threshold energy is still very low, sputtering can be expected to be of minor importance in plasma catalysis.

Etching

Etching, finally, does not require a minimum kinetic energy, but rather requires the formation of a volatile compound through a chemical reaction between the impinging species and the surface species. In this sense, any Eley–Rideal-like process (including hot precursor atom induced desorption) could be considered as an etching process. This is shown in Fig. 9d.

Heating

Possible heating of the catalyst-carrying substrate is highly important, for several reasons. First, the operative temperature of the surface determines the overall catalyst activity to a large extent. Second, the substrate temperature also influences the elementary processes such as adsorption, diffusion, chemical surface reactions and desorption of surface species. Third, the occurrence of so-called hot-spots has in plasma catalysis been proposed as possible cause for an increased catalytic activity.

The issue of catalyst heating is mainly of importance for DBDs [93]. Indeed, in the case of a gliding arc, the gas temperature is in any case sufficiently high to thermally activate the catalyst. In the case of e.g. a cold atmospheric plasma jet, there are essentially no heating mechanisms operative, and plasma-induced thermal activation of the catalyst is excluded. In the case of DBDs, however, the gas temperature is low, but the ions, electrons, electric fields, etc., interact directly with the catalyst surface and may induce a local temperature increase.

Moreover, it is important to note that in DBDs temperature gradients at the surface may arise. This is due to the fact that the heat capacity of metals is typically lower than the heat capacity of most commenly used dielectric support materials and their thermal conductivity is much higher. For instance, Ni has a heat capacity $C_p = 0.44$ J g^{-1} K^{-1}, to be compared to the heat capacity for Al_2O_3 $C_p = 0.72$ J g^{-1} K^{-1} or silica, $C_p = 0.73$ J g^{-1} K^{-1}. The thermal conductivity of Ni is $\kappa = 90.9$ W m^{-1} K^{-1}, to be compared to values of $\kappa = 20$ W m^{-1} K^{-1} and $\kappa = 1.4$ W m^{-1} K^{-1} for Al_2O_3 and silica, respectively. Moreover, several dielectric materials commonly used in DBDs for plasma catalysis such as $BaTiO_3$ and $SrTiO_3$ have high dissipation factors, leading to dielectric loss heating.

Examples of dielectrics with lower dissipation factors include Al_2O_3 and silica, where heating through dielectric loss is of less importance. These effects shall be described below in Sect. 3.6.1.5.

For instance, Holzer et al. [94] noted that in their packed bed reactor using ferroelectric pellets, the macroscopic temperature did not exceed 60 °C, and concluded that the observed ozone decomposition could hence only be explained by the occurrence of local hot spots. The occurrence of hot spots was directly observed by Tirumala et al. [95] in a DBD. This is shown in Fig. 10. The temperature increase in these hot spots, however, was limited to only a few tens of degrees. Hence, while the occurrence of hot spots seems established, their importance is not. Nevertheless, it should be realized that when significant input power is used, the plasma may effectively heat the surface and thereby drastically modify the surface chemistry.

As described in detail by Kersten, the heating of surfaces in low-temperature plasmas is a very complex phenomenon [96]. Indeed, while heat transfer between plasma and the surface in thermal plasmas can be treated by a classical thermal conductivity treatment, involving heat transfer coefficients, this approach does not work well in non-equilibrium low temperature plasmas.

In principle, the overall energy balance at the substrate can be determined from the heat flux (in energy per unit of time) towards the surface, $\dot{Q}_{in}$, and the heat flux originating from the surface, $\dot{Q}_{out}$. These contributions can be written as [96]:

$$Q_{in} = \int (J_{rad,in} + J_{ch} + J_n + J_{exo} + J_{diel} + J_{ext,in}) dA \tag{7}$$

and

$$Q_{out} = \int (J_{rad,out} + J_{conv} + J_{des} + J_{particle,out} + J_{endo} + J_{ext,out}) dA \tag{8}$$

where J_x are the various contributing energy fluxes (in units of energy per unit of time and per unit of area). These contributions include the radiation influx $J_{rad,in}$ and outflux $J_{rad,out}$, the energy flux due to incoming charged (J_{ch}) and neutral (J_n) species, including the heat

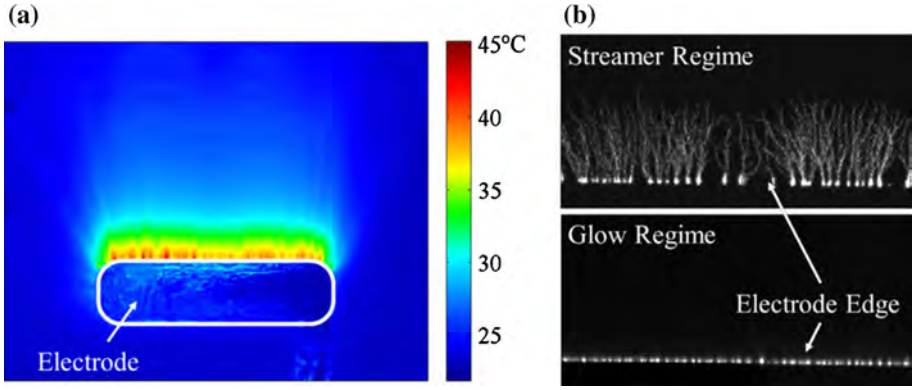

Fig. 10 **a** Absolute temperature distribution in a DBD, showing the occurrence of surface hot spots, and **b** iCCD images of the streamer and glow discharge regimes in a DBD. Reproduced with permission from [95]

release by adsorption and condensation, the heat flux due to exothermic and endothermic surface reactions J_{exo} and J_{endo}, the heat outflux associated with desorption J_{des}, the heat outflux due to sputtered species and secondary electrons $J_{particle,out}$, dielectric heating J_{diel}, and the external heating $J_{ext,in}$ and $J_{ext,out}$. These various terms shall be described below.

Heat Influx

Radiation Heat ($J_{rad,in}$) The heat influx due to radiation is due to radiation emitted by surrounding walls and radiation emitted by the plasma itself. In DBDs, where the operating temperature is usually not very high, the radiation contribution by surrounding walls is probably rather low. The importance of plasma-generated photons, on the other hand, is more difficult to estimate. Photon fluxes ranging from 2.5 μW/cm^2 [80] to 100 μW/cm^2 [97] have been reported. It is not likely that these fluxes are sufficient to significantly heat the surface and hence be of any influence in plasma catalysis.

Energy Influx by Charged Particles (J_{ch}) The total energy flux by charged particles is given as the sum over the various types of particles of their flux times their energy, plus the energy flux by surface recombination of positive ions and electrons. Clearly, this term will only be of any importance in single-stage plasma reactors, since no charge carriers will be present at the catalyst surface in a two-stage setup. In constrast, in discharges where a large electric field is present near the surface, as is the case for DBDs, charge carriers may contribute significantly to the total energy transfer.

The energy contribution of the ions consists of a kinetic part and a potential energy part. The kinetic energy of the ion is characterized by the ion energy distribution function (IEDF), and determined by the sheath potential and the collisional processes in the sheath. While in low pressure RF-excited plasmas saddle shaped IEDFs occur, showing a high probability at high energies, atmospheric pressure plasmas such as the DBDs used in plasma catalysis do not show such high energy ions. In this case, the average ion energy is in the order of perhaps only a few eV, and hence likely to be of little importance in heating the surface.

The contribution of the potential energy depends on the surface material. In the case of an insulating or dielectric surface, the potential energy is due to the adsorption energy $E_{i,ads}$ of the ion in addition to the ion–electron recombination energy:

$$E_{i,pot,diel} = E_{rec} + E_{i,ads} \tag{9}$$

Especially on dielectrics such as glass, as often used in DBDs, the recombination energy is of major importance for surface heating. In the case of metallic surfaces, on the other hand, the neutralization of the impinging ion is accompanied by the emission of secondary electrons. In this case, the ion potential energy is given by [96]:

$$E_{i,pot,metak} = E_{ip} - \Phi - \gamma_i(\Phi + E_{i,kin}) \tag{10}$$

where E_{ip} is the ionization potential of the impinging ion, Φ is the metal work function, γ_i is the secondary electron yield and $E_{ion,kin}$ is the kinetic energy of the impinging ion.

Heating due to electron impact is probably of minor importance in plasma catalysis, since in a single-stage setup the electrons need to overcome the plasma potential with respect to the surface (and the bias voltage if any) in order to reach the surface, while they are completely absent in a two-stage configuration.

Energy Influx by Neutral Particles (J_n) In general, also neutral species contribute to the total heat balance through interaction with the surface. This energy flux can be decomposed in energy due to kinetic energy transfer and due to potential energy transfer. The potential energy transfer, in turn, includes the heat of adsorption, heat of condensation and internal excitation potential energy terms (vibrational and electronic excitation).

The kinetic energy term is simply the thermal energy and hence this term is small in low temperature sources. Their potential energy, on the other hand, is distributed over the various vibrational modes, as well as in the electronically excited states, and may be significant.

Neutral species in their vibrational and electronic ground state contribute essentially only through adsorption, in which case the association influx J_{ads} is given by

$$J_{ads} = j_n \gamma E_{ads} = \frac{1}{4} \gamma n_{exc} \sqrt{\frac{8kT_g}{\pi m}} E_{ads} \tag{11}$$

where j_n is the flux of neutrals, γ is the sticking coefficient, T_g is the gas temperature, and E_{ads} is the heat of adsorption. The mechanistic aspects of the adsorption process were described above in Sect. 3.1.1.

If the neutral is electronically excited, it may transfer part of this excitation energy to the surface with a probability ξ. The total energy flux is then given by

$$J_{exc} = \frac{1}{4} \xi n_{exc} \sqrt{\frac{8kT_g}{\pi m}} E_{exc} \tag{12}$$

where n_{exc} is the density of the exited species under consideration, and E_{exc} is the excitation energy. Although the probability ξ is typically in the order of 0.1–1 (except for low-lying metastable O_2 levels), electronically excited species will generally not contribute significantly to surface heating in plasma catalysis.

Neutral molecules may also be vibrationally excited. However, the electron energy in DBDs is somewhat too high for efficient excitation of the vibrational levels [98], and these species are therefore not likely be of major importance in heating the surface. Moreover, the life time of vibrationally excited species at atmospheric pressure is too low to be of any significance in gliding arcs as well. We may therefore conclude that the contribution of neutral species to the catalyst heating will be almost exclusively due to (exothermic) adsorption, rather than due to their kinetic energy or vibrational excitation.

Energy Influx by Exothermic Surface Reactions (J_{exo}) The heat released in an exothermic surface reaction contributes to the surface heating. The extent of this contribution is, of course, determined by the exact processes. This heating process consists of various underlying processes. These underlying processes are described in Sect. 3.1.1. As mentioned in Sect. 3.1.1, the heat may be dissipated through the excitation of phonons (i.e., the actual heating of the surface), but also through the emission of charged particles (electrons), photons, and the formation of electron–hole pairs. Moreover, if volatile product molecules are formed, these species may desorb from the surface, possibly with internal excitation (vibration and rotation). Hence, part of the heat released during the exothermic surface reaction may also be transferred to the desorbing molecules.

Dielectric Heating (J_{diel}) Dielectric heating is the heating of a dielectric material in response to an alternating electric field. The polar molecules try to line up with the field, and this leads to heating.

The generated power density per volume is given by:

$$Q = \omega \cdot \varepsilon_r'' \cdot \varepsilon_0 \cdot E^2 \tag{13}$$

where ω is the angular frequency of the electromagnetic radiation, ε_r'' is the complex part of the relative permittivity, ε_0 is the relative permittivity of free space and E is the electric field strength. Hence, in order for dielectric heating to be efficient, sufficiently high frequencies in the order of MHz or higher are needed. Typical DBDs used for plasma catalysis however work at much lower frequencies, typically in the kHz region.

The material's ability to dissipate electromagnetic energy is characterized by the so-called loss tangent, which (in the absence of free charge conduction) is defined as

$$\tan\delta = \frac{\varepsilon''}{\varepsilon'} \tag{14}$$

where ε_r' is the real part of the relative permittivity. The total relative permittivity is then defined as

$$\varepsilon = \varepsilon' - i\varepsilon'' \tag{15}$$

An often used dielectric in plasma catalysis is $BaTiO_3$, which incidentally shows a rather weak frequency dependence for the loss tangent [99]. The loss tangent for $BaTiO_3$ is rather high, about 0.02 [99, 100]. Hence, it is not excluded that heating through dielectric loss is an important heating mechanism in plasma catalysis by DBDs.

Heat Outflux

Radiation Heat ($J_{rad,out}$) In the absence of external cooling, thermal radiation is typically the dominant substrate cooling mechanism. The power dissipated from the surface through radiation can be determined from Stefan's Law:

$$\int J_{rad,out} dA = A_s \sigma (\varepsilon_s T_s^4 - \varepsilon_{env} T_{env}^4) \tag{16}$$

where A_s is the total radiation emitting surface of the substrate, σ is the Stefan-Boltzmann constant, ε_s and ε_{env} are the emissivities of the substrate and the environment, respectively, and T_s and T_{env} are the substrate surface temperature and environmental temperature, respectively. The emissivity of the environment is typically assumed ≈ 1. For the substrate, the emissivity of typical catalyst materials such as Ni or Cu is in the order $\varepsilon_s = 0.02$–0.1, while for dielectric materials such as glass, $\varepsilon_s \approx 0.9$ [96].

Thermal Conduction (J_{cond}) Substrate cooling though thermal conduction, separate from external cooling, consists of heat exchange with the impinging gas molecules. In the collisional regime, which is the typical regime in atmospheric pressure discharges, the mean free path of the gas molecules is much shorter than the thermal boundary layer d_{sh}. At atmospheric pressure and room temperature, the mean free path is in the order of 50–100 nm, which is similar to or perhaps one order of magnitude larger than typical catalyst surface features. In this case, the heat flux density is given by:

$$\int J_{cond} dA = N_u \lambda_g d_{sh} (T_s - T_g) \tag{17}$$

where N_u is the Nusselt number, λ_g is the thermal conductivity of the gas, d_{sh} is the thermal boundary layer in front of the substrate, and T_s and T_g are the substrate and gas temperatures, respectively.

Thermal Desorption (J_{des}) Thermal desorption is a key process in plasma catalysis for numerous processes including natural gas reforming, VOC abatement and ammonia production. In other plasma catalytic processes, such as carbon nanotube growth, desorption is of much less importance. Thermal desorption may occur through either of four basic mechanisms: physical sputtering (PS, discussed in Sect. 3.5.3), chemical etching (CE, discussed in Sect. 3.5.4), surface film reaction (SFR, discussed in Sect. 3.3), and desorption following electronic excitation (discussed in Sect. 3.2.2.4). In chemical etching, incoming particles are usually considered to react with surface species through the Eley–Rideal mechanism, forming volatile molecules. These volatile species may subsequently desorb, either directly, or after some delay. In surface film reaction, surface species react with each other through a Langmuir–Hinshelwood mechanism, and subsequently desorb. Either way, however, desorption usually consists of molecules leaving the surface with an energy comparable to the surface temperature.

(i.e., desorbing molecules are usually in thermal equilibrium with the surface), irrespective of the mechanism by which the molecule was formed. Although the desorbing molecule may contain some internal excitation energy, thermal desorption does not contribute significantly to the total heat outflux.

Endothermic Surface Reactions (J_{endo}) Endothermic surface reactions may occur either through desorption (described in the previous section) or through chemical surface reactions which do not lead to desorption. The latter are of crucial importance in for instance gas reforming, where the feedstock needs to be converted in the desired product molecules through the formation of a series of surface-bound intermediates. The overall reaction enthalpy, which according to Hess' Law is equal to the sum of the reaction enthalpies of the individual elementary processes, is then the quantity of interest. The importance of the reaction enthalpy with respect to surface cooling is thus determined by the specific targetted reaction, and independent of the plasma.

Particle Emission ($J_{particle}$) Another heat loss channel is the emission of neutral and charged particles from the surface. For particle emission to occur, some threshold energy needs to be overcome, corresponding to the binding energy of the particle to the surface. Note that the energy loss through the emission of secondary electrons due to (slow) incoming ions is already accounted for by Eq. (10), and this process should hence not be included in $J_{particle}$. However, while other emission processes, leading to the emission of neutral and ionic species from the surface, are of great importance in low pressure plasmas, where the non-negligible fraction of the impinging particles have sufficient energy to deliver the threshold energy, they are generally of little concern in atmospheric pressure discharges given the low energies of the impinging particles.

External Heating ($J_{ext,in}$ and $J_{ext,out}$)

External heating and cooling of the substrate occur through conduction. The mechanism of this process is phonon excitation.

External heating or cooling can be applied to the substrate, and it is then often assumed that the substrate surface temperature corresponds to the externally controlled temperature. However, the actual surface temperature depends on the thermal conductivity and the thickness of the substrate, determining how fast the externally set temperature can be coupled to the substrate surface, and the time scale of the surface processes.

Indeed, the energy of phonons is typically in the meV order, which is several orders of magnitude lower than chemical reaction energies. Hence, heat dissipation through the substrate lattice requires multiple phonon excitations, which may not occur instantaneously. Hence, hot spots may temporarily occur.

Surface Discharge Formation

Since the combination of the plasma with a catalyst is usually intended to result in a synergistic effect, it is beneficial to create a strong discharge over the entire catalyst-covered surface. A surface discharge can be formed as a thin layer covering the dielectric surface in a DBD. A nice example of exciting a surface discharge in the context of plasma catalysis was provided by Kim [22]. In these experiments, packing the discharge volume with zeolite pellets, covered by Ag nanoparticles, was shown to greatly enhance the plasma generation on the surface. Hence, the Ag nanoparticles were key for surface streamers to develop and spread over the catalyst surface. In the case of $BaTiO_3$ pellets, however, partial discharges were formed (at the contact points of the $BaTiO_3$ beads), but surface streamers were not observed [22].

Tu et al. [33] observed that depending on the packing conditions, a volume discharge may change into a surface discharge. The relation between packing conditions and discharge mode, however, is complex, and the relative contribution of surface discharge versus filamentary discharge was found to depend on the particle size, particle shape and packing location [33].

Electric Field Enhancement

Electric field enhancement by the presence of a packing in the plasma reactor is well known. Two fundamental causes for this field enhancement can be distinguished. First, the electric field is naturally enhanced near tip-like structures, an effect termed the "lighting rod effect", which is a manifestation of an electric edge effect. The resulting local electric field E near the tip can generally be described by.

$$E = \beta E_0 \tag{18}$$

where E_0 is the global electric field, and β is the so-called field enhancement factor. The enhancement factor ranges from 1 for a flat surface to thousands for high aspect ratio structures such as carbon nanotubes. Typical surface features may show factors of a few tens to hundreds. The lightning rod effect is a pure shape effect: electric field lines must terminate normal to the surface of a conductor, and hence the electric field lines tend to concentrate near sharp points of highly conductive materials such as the metallic nanoparticles usually used in plasma catalysis.

The field enhancement factor is a function of the exact shape of the tip-like structure. In the case that the tip can be approximated by a elliptical paraboloid, the electric field relative to its maximum value E_{max} at the apex can be expressed as [101]:

$$E = \frac{E_{\max}}{\sqrt{1 + \frac{r^2}{R^2}}} \tag{19}$$

where r is the radial distance from the axis of cylindrical symmetry of the paraboloid, and R is the radius of curvature at the apex. Hence, at the apex, $r = 0$, and $E = E_{max}$. For elongated structures such as CNTs, the field enhancement factor can in a first approximation be written as

$$\beta \cong \frac{h}{d} \tag{20}$$

where h is the height of the tube and d is its diameter.

The second effect is related to the so-called packed bed effect. Often, DBDs are filled or partially filled with dielectric beads to improve the plasma catalytic process. The relative permittivity (or dielectric constant) of the dielectric material used for the beads then codetermines the electric field enhancement.

The electric field enhancement due to the packing effect can be described as [102, 103]:

$$E = \frac{V}{d}\frac{3\varepsilon_p}{2\varepsilon_p + \varepsilon_g} \tag{21}$$

where d is the gap length, and ε_p and ε_g are the (real parts of the) relative permittivities of the beads and the gas, respectively. Hence, given a sufficiently large relative permittivity of the packing material, an enhancement factor up to 1.5 can be obtained. However, it is important to realize that this formula was derived for a spherical void, whereas the voids in a packed bed reactor are not spherical. This may limit the applicability of this formula.

The physical origin of this effect is the spontaneous polarization occurring in the ferroelectric material in response to the existance of an external electric field. This in turn results in a high electric field at the contact points on the pellets, which induce electrical discharges near these points [26]. The actual field enhancement may amount to a factor of 10–250, depending on the shape, porosity and dielectric of the pellets [43], which is significantly larger that the enhancement predicted by Eq. (20). Very recent detailed calculations indeed demonstrated such large enhancement factors, as shown in Fig. 11, for a packed bed dielectric barrier discharge at 300 K and 1 atm in He [104].

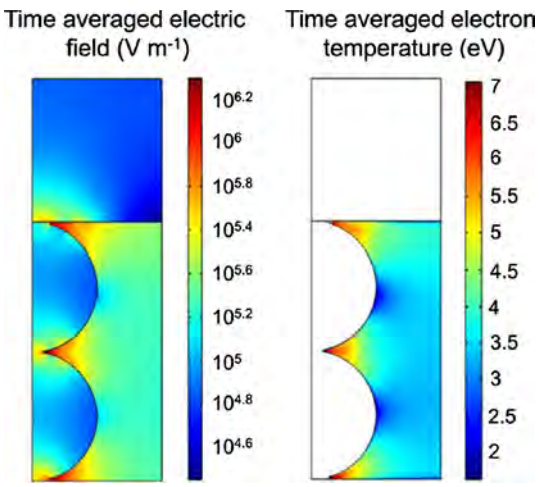

Fig. 11 Calculated (*left panel*) time averaged electric field and (*right panel*) time averaged electron temperature, showing the significant field enhancement and electron temperature resulting from the packed bed effect. Reproduced with permission from [104]

Conclusions

In this review, a wide variety of plasma-surface interactions are discussed in the context of plasma catalysis. Focussing on atmospheric pressure dielectric barrier discharges (DBD) and gliding arcs as two very different types of reactors experimentally used in plasma catalysis, the importance of these interactions is assessed. Especially in DBDs the strong non-equilibrium nature of the discharge complicates the analysis. It is concluded that some factors previously regarded as key factors are perhaps of less importance, including photon-induced photocatalyst activation and hot spot formation at the catalyst surface. Other factors such as electric field enhancement and hot precursor induced surface reactions, on the other hand, are expected to be of major importance. It is clear that many of the processes and plasma-surface interactions discussed in this review have not yet been investigated in great detail in the context of plasma catalysis. The combination of experimental, theoretical and modeling studies is warranted to advance the field and gain a more fundamental insight in the operative mechanisms than currently available.

Acknowledgments The author is indebted to many colleagues for fruitful discussions. In particular discussions with A. Bogaerts (University of Antwerp, Belgium), H.-H. Kim (AIST, Japan), J. C. Whitehead (University of Manchester, UK) and T. Nozaki (Tokyo Institute of Technology, Japan) are greatfully acknowledged and appreciated.

References

1. Whitehead JC (2010) Pure Appl Chem 82:1329–1336
2. Tatarova E, Bundaleska N, Sarrette JP, Ferreira CM (2014) Plasma Sources Sci Technol 23:063002
3. Jõgi I, Erme K, Haljaste A, Laan M (2013) Eur Phys J Appl Phys 61:24305
4. Maciuca A, Batiot-Dupeyrat C, Tatibouët JM (2012) Appl Catal B Environ 125:432–438
5. Kim HH, Ogata A, Schiorlin M, Marotta E, Paradisi C (2011) Catal Lett 141:277–282
6. Nozaki T, Tsukijihara H, Fukui W, Okazaki K (2007) Energy Fuels 21:2525–2530
7. Nozaki T, Goujard V, Yuzawa S, Moriyama S, Agiral A, Okazaki K (2011) J Phys D Appl Phys 44:274010
8. Bromberg L, Cohn DR, Rabinovich A, Alexeev N (1999) Int J Hydrog Energy 24:1131–1137
9. Futamura S, Kabashima H, Annadurai G (2006) Catal Today 115:211–216
10. Mei E, Zhu X, He Y, Yan JD, Tu X (2015) Plasma Sources Sci Technol 24:015011
11. Kumar V, Kim JH, Jasinski JB, Clark EL, Sunkara MK (2011) Cryst Growth Des 11:2913–2919
12. Kato T, Hatakeyama R (2012) Nature Nanotech 7:651–656
13. Ostrikov K, Levchenko I, Cvelbar U, Sunkara M, Mozetic M (2010) Nanoscale 2:2012–2027
14. Wang L, Zhao Y, Liu C, Gong W, Guo H (2013) Chem Commun 49:3787–3789
15. Sobacchi MG, Saveliev AV, Fridman AA, Kennedy LA, Ahmed S, Krause T (2002) Int J Hydrog Energy 27:635–642
16. Mingdong B, Xiyao B, Zhitao Z, Mindi B (2000) Plasma Chem Plasma Proc 20:511–520
17. Mizushima T, Matsumoto K, Ohkita H, Kakuta N (2007) Plasma Chem Plasma Proc 27:1–11
18. Kim HH, Teramoto Y, Negishi N, Ogata A (2015) Catal Today 256:13–22
19. Neyts EC, Bogaerts A (2014) J Phys D Appl Phys 47:224010
20. Ostrikov K, Neyts EC, Meyyappan M (2013) Adv Phys 62:113–224
21. Neyts EC (2012) J Vac Sci Technol B 30:030803
22. Kim HH (2011) Eur Phys J Appl Phys 55:13806
23. Meyyappan M (2009) J Phys D Appl Phys 42:213001
24. Chen HL, Lee HM, Chen SH, Chao Y, Chang MB (2008) Appl Catal B Environ 85:1–9
25. Van Durme J, Dewulf J, Leys C, Van Langenhove H (2008) Appl Catal B Environ 78:324–333
26. Kim HH (2004) Plasma Process Polym 1:91–110
27. Zhang AJ, Zhu AM, Guo J, Xu Y, Shi C (2010) Chem Eng J 156:601–606
28. Demidyuk V, Whitehead JC (2007) Plasma Chem Plasma Process 27:85–94
29. Tu X, Gallon HJ, Twigg MV, Gorry PA, Whitehead JC (2011) J Phys D Appl Phys 44:274007

30. Sentek J, Krawczyk K, Mlotek M, Kalczewska M, Kroker T, Kolb T, Schenk A, Gericke KH, Schmidt-Szalowski K (2010) Appl Catal B Environ 94:19–26
31. Tu X, Whitehead JC (2014) Int J Hydrog Energy 39:9658–9669
32. Tu X, Whitehead JC (2012) Appl Catal B Environ 125:439–448
33. Tu X, Gallon HJ, Whitehead JC (2011) J Phys D Appl Phys 44:482003
34. Neyts EC, Ostrikov K (2015) Catal Today 256:23–28
35. Klasovsky F, Claus P (2008) Metal nanoclusters in catalysis: effects of nanoparticle size, shape and structure. In: Corain B, Schmid G, Toshima N (eds) Metal nanoclusters in catalysis and materials science: the issue of size control, chapter 8. Amsterdam, Elsevier
36. Huu TP, Gil S, Da Costa P, Giroir-Fendler A, Khacef A (2015) Catal Today. doi:10.1016/j.cattod.2015.03.001
37. Kogelschatz U (2003) Plasma Chem Plasma Process 23:1–46
38. Wagner H-E, Brandenburg R, Kozlov KV, Sonnenfeld A, Michel P, Behnke JF (2003) Vacuum 71:417–436
39. Pappas D (2011) J Vac Sci Technol A 29:020801
40. Xu X (2001) Thin Solid Films 390:237–242
41. Belmonte T, Arnoult G, Henrion G, Gries T (2011) J Phys D Appl Phys 44:363001
42. Babaeva NY, Kushner MJ (2013) J Phys D Appl Phys 46:025401
43. Fridman A (2012) Plasma chemistry. Cambridge University Press, New York
44. Lie L, Bin W, Chi Y, Chengkang W (2006) Plasma Sci Technol 8:653–655
45. Allah ZA, Whitehead JC (2015) Catal Today 256:76–79
46. Lee H, Sekiguchi H (2011) J Phys D Appl Phys 44:274008
47. Fridman A, Nester S, Kennedy LA, Saveliev A, Mutaf-Yardimci O (1999) Prog Energy Combust Sci 25:211–231
48. Yang YC, Lee BJ, Chun YN (2009) Energy 34:172–177
49. Ruban A, Hammer B, Stoltze P, Skriver HL, Nørskov JK (1997) J Molec Catal A Chem 115:421–429
50. Hammer B, Nørskov JK (2000) Adv Catal 45:71–129
51. Groß A (2003) Chem Phys Solid Surf 11:1–26
52. Ertl G (2000) Adv Catal 45:1–69
53. Bronold FX, Deutsch H, Fehske H (2009) Eur Phys J D 54:519–544
54. Ambrico PF, Ambrico M, Schiavulli L, Ligonzo T, Augelli V (2009) Appl Phys Lett 94:051501
55. Ambrico PF, Ambrico M, Colaianni A, Schiavulli L, Dilecce G, De Benedictis S (2010) J Phys D Appl Phys 43:325201
56. Guaitella O, Thevenet F, Guillard C, Rousseau A (2006) J Phys D Appl Phys 39:2964–2972
57. Herschleb CT (2011) Ph.D. Thesis, Casimir Ph.D. series, Delft-Leiden, The Netherlands
58. Haddou N, Ghezzar MR, Abdelmalek F, Ognie S, Addou A (2013) Plasma Sci Technol 15:915–922
59. Cacciatore M, Rutigliano M (2009) Plasma Sources Sci Technol 18:023002
60. Rettner CT, Auerbach DJ, Lee J (1996) J Chem Phys 105:10115
61. Doornkamp C, Ponec V (2000) J Molec Catal A Chem 162:19–32
62. Vannice MA (2007) Catal Today 123:18–22
63. Dombrowski E, Peterson E, Del Sesto D, Utz AL (2015) Catal Today 244:10–18
64. Lee MB, Yang QY, Ceyer ST (1987) J Chem Phys 85:1693
65. Lee MB, Yang QY, Ceyer ST (1987) J Chem Phys 87:2724
66. Smith RR, Killelea DR, DelSesto DF, Utz AL (2004) Science 304:992–995
67. Juurlink LBF, Smith RR, Killelea DR, Utz AL (2005) Phys Rev Lett 94:208303
68. Beckerle JD, Yang QY, Johnson AD, Ceyer ST (1987) J Chem Phys 86:7236–7237
69. Beckerle JD, Johnson AD, Yang QY, Ceyer ST (1989) J Chem Phys 91:5756–5777
70. Åkerlund C, Zorić I, Kasemo B (1996) J Chem Phys 104:7359
71. Vattuone L, Gambardella P, Burghaus U, Cemic F, Cupolillo A, Valbusa U, Rocca M (1998) J Chem Phys 109:2490–2502
72. Bonn M, Funk S, Hess C, Denzler D, Stampfl C, Scheffler M, Wolf M, Ertl G (1999) Science 285:1042
73. Hertel T, Wolf M, Ertl G (1995) J Chem Phys 102:3414
74. Polanyi M, Wigner E (1928) Z Phys Chem Abt A 139:439
75. Kang M, Kim BJ, Cho SM, Chung C-H, Kim BW, Han GY, Yoon KJ (2002) J Mol Catal A Chem 180:125–132
76. Kim HH, Lee YH, Ogata A, Futamura S (2003) Catal Commun 4:347–351
77. Diesen V (2011) Ph.D. Thesis, Stockholm, Sweden
78. Lee BY, Park SH, Lee SC, Kang M, Choung SJ (2004) Catal Today 93–95:769–776
79. Yu S, Liang Y, Sun S, Zhang K, Zhang J, Fang J (2013) PLoS One 8:e59974
80. Sano T, Negishi N, Sakai E, Matsuzawa S (2006) J Mol Catal A Chem 245:235–241

81. Rousseau A, Guaitella O, Gatilova L, Thevenet F (2005) Appl Phys Lett 87:221501
82. Thevenet F, Guaitella O, Puzenat E, Herrmann JM, Rousseau A, Guillard C (2007) Catal Today 122:186–194
83. Lee J, Sorescu DC, Deng X (2011) J Am Chem Soc 133:10066–10069
84. Tan S, Zhao J, Wang Z, Ma C, Zhao A, Wang B, Luo Y, Yang J, Hou J (2011) Phys Rev B 84:155418
85. Zhao A, Tan S, Li B, Wang B, Yang J, Hou JG (2013) Phys Chem Chem Phys 15:12428–12441
86. Somers W, Bogaerts A, van Duin ACT, Neyts EC (2012) J Phys Chem C 116:20958–20965
87. Somers W, Bogaerts A, van Duin ACT, Huygh S, Bal KM, Neyts EC (2013) Catal Today 211:131–136
88. Kim HH, Tsubota S, Daté M, Ogata A, Futamura S (2007) Appl Catal A Gen 329:93–98
89. Sivachandrian L, Thevenet F, Gravejat P, Rousseau A (2013) Chem Eng J 214:17–26
90. Mok YS, Jwa E, Hyun YJ (2013) J Energy Chem 22:394–402
91. Baraton L, He Z, Lee CS, Maurice JL, Cojocaru CS, Gourgues-Lorenzon AF, Lee YH, Pribat D (2011) Nanotechnology 22:085601
92. Eckstein W, Garcia-Rosales C, Roth J (1993) Nucl Instrum Methods Phys Res B 83:95–109
93. Jidenko N, Bourgeois E, Borra JP (2011) J Phys D Appl Phys 43:295203
94. Holzer F, Kopinke FD, Roland U (2005) Plasma Chem Plasma Process 25:595–611
95. Tirumala R, Benard N, Moreau E, Fenot M, Lalizel G, Dorignac E (2014) J Phys D Appl Phys 47:255203
96. Kersten H, Deutsch H, Steffen H, Kroesen GMW, Hippler R (2001) Vacuum 63:385–431
97. Rajasekaran P, Mertmann P, Bibinov N, Wandke D, Viöl W, Awakowicz P (2010) Plasma Process Polym 7:665–675
98. Bogaerts A, Kozak T, Van Laer K, Snoeckx R (2015) Farad Dis. doi:10.1039/C5FD00053J
99. Tohma T, Masumoto H, Goto T (2002) Mater Trans 43:2880–2884
100. Wodecka-Dus B, Czekaj D (2009) Arch Metall Mater 54:923–933
101. Gaspard P (2012) In: Mikhailov AS, Ertl G (eds) Proceedings of the international conference "engineering of chemical complexity", Berlin Center for Studies of Complex Chemical Systems, World Scientific, Singapore, 4–8 July 2011
102. Kim H-H, Ogata A (2012) Int J Plasma Environ Sci Technol 6:43–48
103. Takaki K, Chang JS, Kostov KG (2004) IEEE Trans Dielectrics Electrical Insul 11:481–490
104. Van Laer K, Bogaerts A (2015) Plasma Sources Sci. Technol. submitted